ESOMAT 2009, 03010 (2009)
DOI:10.1051/esomat/200903010

Cu-Al-Ni microstructure in the phenomenological theory of martensite with lattice invariant deformation

A. Ostapovets[a], V. Paidar and N. Zarubova

Institute of physics ASCR v.v.i, Na Slovance 2, 18221 Prague 8, Czech Republic

Abstract. Geometrical analysis of interfaces in a Cu-Al-Ni alloy is performed on the basis of the phenomenological theory of martensite. The austenite-martensite interfaces in the foils of the Cu-Al-Ni alloy are faceted. In order to assess possible facet planes, lattice invariant deformation in the form of a simple shear is included into the phenomenological theory. The experimentally observed normals to the facet planes lie in the predicted regions. Experimentally observed lines in the intervariant interfaces are interpreted as slip steps. The directions of these lines agree with theoretical predictions.

1. Introduction

The Cu–Al–Ni alloy with approximately 14wt%Al and 4wt%Ni belongs to the most widely studied shape memory alloys because of a very large reversible strain and a relative ease of single crystal preparation. The cubic austenite to the orthorhombic martensite phase transition takes place in Cu–Ni–Al alloys. The structure of the parent cubic austenite β_1 phase is of the $D0_3$ type with the lattice parameter a_0=0.5836 nm [1]. Cu–Al–Ni is a ternary alloy but it is considered in the literature as $D0_3$ because Cu and Ni occupy the same sublattice. Three types of martensite are observed in this alloy: γ_1' with 2H, β_1' with 18R and α_1' with 6R structures [2]. The structure of the orthorhombic γ_1' martensite is of Cu_3Ti type with the lattice parameters a=0.4382 Å, b=0.5356 Å, c=0.4222 nm [3]. The 2H martensite with six different orientations can arise from one orientation of the austenite. Two of three orthorhombic axes correspond to the <110> cubic directions and the third one to $\langle 001 \rangle$. The basal plane of the 2H structure arises from a $\{110\}_{\beta_1}$ austenite plane.

An analysis of twin and habit planes in Cu-Al-Ni alloy with 2H martensite in the terms of phenomenological theory can be found for instance in the works of Hane and Shield [4] or Bhattacharya [5]. Theoretically three types of twins are possible in this material: compound twins on $\{101\}_{2H}$ plane, type I twins on $\{121\}_{2H}$ plane and type II twins on irrational near $\{'231'\}_{2H}$ plane. All three types of twins were observed experimentally [6-8]. According to the phenomenological theory of martensites [4, 5, 9] there is no solution for a planar interface separating a single variant of the γ_1' martensite and the austenite in Cu-Al-Ni alloys. Hence the austenite–martensite interface must be constructed using a lattice-invariant deformation (LID). Twinning was taken as LID in Refs. 4, 5. The martensite consists of thin plates of two different martensite variants in this approach. The habit planes in the case of type-I twins were observed experimentally in Ref. 10. The obtained $(331)\beta_1$ plane is close to the theoretical (0.6355, 0.7484, 0.1797)β_1 plane. The measurements for type-II twins were performed [11] and the experimental habit plane is (0.648, 0.725, 0.234)β_1, close to the (0.6350, 0.7275, 0.2599)β_1 theoretical plane.

Faceted austenite-martensite interfaces were observed in the foils of Cu-Al-Ni alloys deformed *in-situ* in transmission electron microscope [12]. The foils were in β_1 austenite at room temperature and transformed to γ_1'(2H) and β_1' martensites under stress. The normal to the foil surface was close to the $[\bar{1}20]\,\beta_1$ direction, and the axis of tension was close to $[63\bar{2}]\,\beta_1$. For more details of the experiment see [12,13]. A typical interface between austenite and γ_1' martensite is shown in Fig. 1. The twin related γ_1'(V1) and γ_1'(V3) martensite variants produce facets on the γ_1'/β_1 interface. Notation of martensite variants introduced in [13] is used. The planes of facets in Fig. 1 are close to $\{331\}\,\beta_1$, but interfaces of other crystallography were found, too (see Fig. 3).

[a]e-mail: ostapov@fzu.cz

Article available at http://www.esomat.org or http://dx.doi.org/10.1051/esomat/200903010

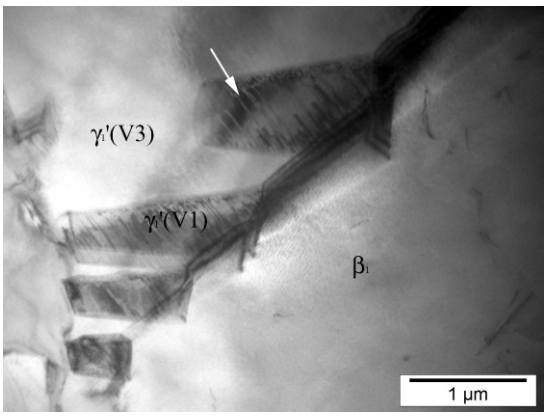

Fig. 1. Faceted austenite-martensite interface with plates of γ_1'(V1) martensite inside γ_1'(V3) martensite variant. The sets of parallel defects (marked by arrow) are present in the intervariant interfaces. According to [12]

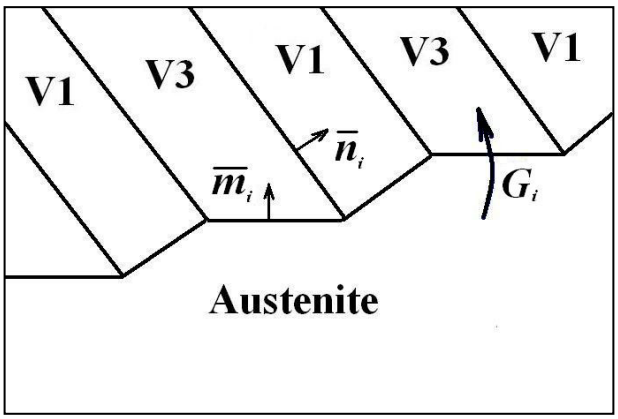

Fig. 2. Illustration of studied configuration. Austenite-martensite interface consists of facets which are planar boundaries between austenite and a single variant of martensite. $\boldsymbol{m_i}$ is the normal to facet plane, $\boldsymbol{n_i}$ is the normal to the intervariant interface, $\boldsymbol{G_i}$ is the matrix describing transformation from the austenite to the *i*-th variant of martensite.

The experimental orientation relationship obtained from the electron microscope observations for V3 variant is $[\bar{1}20]\,\gamma_1' \parallel [\bar{1}31]\,\beta_1$ and $(001)\,\gamma_1' \parallel (101)\,\beta_1$. The observed twin boundary planes between V1 and V3 variants are close to a $\{121\}\,\gamma_1'$ plane. It is a plane of type I twinning in this material. Sets of parallel linear defects are observed in the intervariant boundary. These defects are well visible in Fig. 1. The directions of the defect lines are near $[15\ 7\ \bar{1}]\,\gamma_1'$ in γ_1'(V3) martensite coordinate system or near $[\bar{8}79]\,\beta_1$ in austenite coordinate system.

The interfaces observed in Refs.12,13 are discussed in the present paper in the frames of phenomenological theory of martensite using a lattice invariant deformation in the form of a simple shear. Such type of LID can be produced for instance by slip and it is taken into consideration because the approach used in Refs. 4,5 with LID in the form of twinning is not appropriate to explain the occurrence of the microscopic facets in Cu-Al-Ni.

2. Model description

Let us consider the configuration shown in Fig. 2. The orientation relations for the V1 variant are $[100]\gamma_1' \parallel [01\bar{1}]\beta_1$, $[010]\gamma_1' \parallel [100]\beta_1$ and $[001]\gamma_1' \parallel [011]\beta_1$; and for the V3 variant $[100]\gamma_1' \parallel [10\bar{1}]\beta_1$, $[010]\gamma_1' \parallel [010]\beta_1$ and $[001]\gamma_1' \parallel [101]\beta_1$, see [12,13]. These lattice correspondences define transformation stretch matrices (see Ref. 5) U_1 and U_3 for the two of six possible martensite variants.

In our model, the whole austenite–martensite transformation G_i is split into three parts: a homogeneous cubic-to-orthorhombic transformation which is represented by a symmetrical matrix U_i, a simple shear LID S_i, and a rotation R_i. On the other hand, any linear transformation can be decomposed mathematically to a product of orthogonal and symmetrical transformations. Thus $Q_iV_i = R_iS_iU_i$ where V_i is the symmetrical part and Q_i is the orthogonal part (rotation) of the transformation from the austenite to the *i*-th variant of martensite.

Three equations for the kinematical compatibility conditions [4,5] on the boundaries between the austenite and variant V1, the austenite and variant V3, and between the V1 and V3 variants can be written as:

$$Q_1V_1 - I = \boldsymbol{b_1} \otimes \boldsymbol{m_1} \tag{1}$$

$$Q_3V_3 - I = \boldsymbol{b_3} \otimes \boldsymbol{m_3} \tag{2}$$

$$Q_1V_1 - Q_3V_3 = \boldsymbol{a} \otimes \boldsymbol{n} \tag{3}$$

where $\boldsymbol{b_1}$, $\boldsymbol{b_3}$, and $\boldsymbol{a}$ are so-called shape strains which give the magnitude and sense of the transformations, $\boldsymbol{m_1}$, $\boldsymbol{m_3}$ are the normals to the corresponding facet planes, $\boldsymbol{n}$ is the normal to the inter-variant interface and I is the

identity matrix. Let $\boldsymbol{p_i}$ be the unit normal to a plane of shear, $\boldsymbol{s_i}$ the unit vector in the shear direction, and σ a shear magnitude. Then $S_i = I + \boldsymbol{s_i} \otimes \sigma \boldsymbol{p_i}$.

The conditions for the existence of solutions of Eqs. (1) and (2) are that one eigenvalue of the matrices $V_1^{\mathrm{T}}V_1$ and $V_3^{\mathrm{T}}V_3$, respectively, is equal to 1, another one is smaller than 1, and the last one greater than 1 [5]. For Eq. (3), these conditions are similar but the eigenvalues of the matrix $V_1^{-1}V_3^{\mathrm{T}}V_3V_1^{-1}$ are considered.

Equations 1-3 were solved numerically [14]. Different possible simple shear matrices S were examined in order to find solutions. The matrices S were chosen in the following way: $\boldsymbol{p}$ was taken from the unit hemisphere with 0.6° steps, $\boldsymbol{s}$ was taken in the plane with normal $\boldsymbol{p}$ with 0.6° steps and σ was taken in the range from 0 to 0.15 with steps of 0.001. The conditions for the existence of a solution were verified after substitution of S into the equations (1)-(3).

3. Results and discussion

The solutions of Eq. 2 for the variant V3 are shown in Fig. 3. Possible facet planes concentrate in comparatively compact ranges. Fig. 3 represents the case where $\boldsymbol{b_1} \parallel \boldsymbol{b_3}$. Solutions which correspond to the case where $\boldsymbol{m_1} \parallel \boldsymbol{m_3}$, exist, too. These solutions are not presented here because they mean that the facets are parallel and the interface is flat, which does not correspond to the experimental data. The experimental facet planes lie inside the dense region of calculated points in Fig. 3. A similar pattern can be obtained for the V1 variant by a 180° rotation around the $[1\bar{1}0]\beta_1$ axis. The parameters yielded by Eqs. (1),(2) for the facets near $\{331\}\beta_1$ are given in Table 1. Eq. (3) has the solution $\boldsymbol{n}$ = [0.707 -0.707 0.000]β_1 and $\boldsymbol{a}$ = [0.255, 0.255, 0.020] β_1 in this case. The plane with the normal $\boldsymbol{n} = [1\bar{1}0]\beta_1$ coincides with one of the $\{121\}\gamma_1'$ planes in the martensite, which are the twin planes of type-I twinning.

The line defects in Fig. 1. can be interpreted as slip steps in the intervariant boundary. The direction of the defects have to be intersection lines of the shear plane and plane of intervariant boundary in the frame of our theory. It follows from the data in Table 1 that the direction of the linear defects is close to $[\,72\ 72\ \bar{7}9\,]\,\beta_1$ if V1-V3 boundary is considered. This direction is inclined from the experimental one $[8\bar{7}9]\,\beta_1$ by approximately 4° (see Fig. 4). This deviation lies under the value of the experimental error.

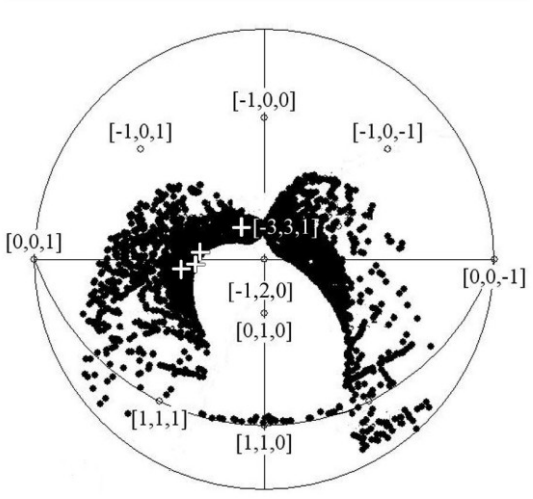

Fig. 3. $[\bar{1}20]$ stereographic projections of austenite. Calculated normals to the facet planes between austenite and γ_1' (V3) martensite variant are shown as black circles. They are solutions of eq. (2) for all possible matrices of a simple shear with the shear magnitude from 0 to 0.15 for the case $\boldsymbol{b_1} \parallel \boldsymbol{b_3}$ The experimental normals to the facet planes are shown as white crosses [12].

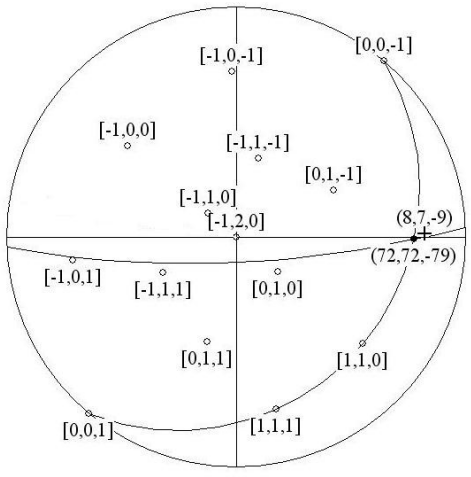

Fig. 4. $[\bar{1}20]$ stereographic projection of austenite. Calculated and experimental direction of slip steps in the V1-V3 intervariant boundary is shown as black point and black cross respectively. The traces of $(1\bar{1}0)$ plane and (-0.689, -0.103, -0.716) shear plane are shown as well.

Table 1. Solutions of Eqs. (1),(2) for facet planes close to $\{331\}\beta_1$

	V1	*V3*
Normal to shear plane, $\boldsymbol{p}$	[0.108, 0.709, 0.697]	[-0.689, -0.103, -0.716]
Shear direction, $\boldsymbol{s_i}$	[-0.313, 0.689, -0.653]	[-0.693, 0.382, 0.611]
Shear value, σ	0.1	0.1
Normal to facet plane, $\boldsymbol{m_i}$	[-0.691, 0.687 , -0.224]	[-0.687, 0.691, 0.224]
Shape strain, $\boldsymbol{b_i}$	[0.131, 0.131, 0.011]	[-0.131, -0.131, -0.011]

4. Conclusions

Possible orientations of austenite–martensite interfaces were calculated in the frame of a model based on the phenomenological theory of martensite with a lattice-invariant deformation in the form of a simple shear. The results of the calculations were compared with the observations on Cu-Al-Ni foils deformed *in situ* in the transmission electron microscope. It was found that the normals to possible facet planes are concentrated in compact regions containing the experimental points. Experimentally observed lines in the intervariant interfaces are interpreted as slip steps. The directions of these lines agree with theoretical predictions.

This research was supported by the COST program P19 OC09014 and by the Grant Agency of AS CR (contracts No. A200100627 and IAA100100920)

References

[1] K. Otsuka, K. Shimizu, Jpn. J. Appl. Phys. **8**, 1196 (1969)
[2] K. Otsuka, H, Sakamoto, K. Shimizu, Acta Met., **27**, 585 (1979)
[3] K. Otsuka, K. Shimizu, Mater. Trans. JIM, **15**, 103 (1974)
[4] K. F. Hane, T. W. Shield, J. Elasticity, **59**, 267 (2000)
[5] K. Bhattacharya, *Microstructure of martensite: why it forms and how it gives rise to the shape-memory effect.* (Oxford University Press, Oxford, 2003)
[6] N. Otani, Y. Funatsu, S. Ichinose, S. Miyazaki, K. Otsuka, Scripta Metall. **17**, 745 (1983).
[7] K. Otsuka, K. Shimizu, J. Phys. Soc. Japan, **28**, 804 (1970)
[8] S. Ichinose, Y. Funatsu, K. Otsuka: Acta Metall. Mater., **33**,1613 (1985)
[9] C. M. Wayman, *Introduction to the crystallography of martensitic transformations* (The Macmillan Company, New York, 1964)
[10] K. Otsuka, K. Shimizu, Trans. Japan. Inst. Metals., **15** 103 (1974)
[11] K. Okamoto, S. Ichinose, K. Morii, K. Otsuka, K. Shimizu, Acta. Metall. Mater. **34**, 2065 (1986)
[12] N. Zarubova, J. Gemperlova, A. Gemperle, Z. Dlabacek, "In-situ TEM study of stress-induced transformations in CuAlNi", ESOMAT 2009, Prague, 7-11 September 2009.
[13] N. Zarubova, J. Gemperlova, V. Gartnerova, A. Gemperle, Mater. Sci. Eng. A **481-482**, 457 (2008)
[14] A. Ostapovets, V. Paidar, N. Zarubova, Int. J. Mat. Res. **100**, 342 (2009)